Enhanced loading of doxorubicin into polymeric micelles by a combination of ionic bonding and hydrophobic effect, and the pH-sensitive and ligand-mediated delivery of loaded drug

Zhenhua Xu [a], Miao Guo [a], Husheng Yan [a,*], Keliang Liu [b,*]

[a] Key Laboratory of Functional Polymer Materials, Ministry of Education, Institute of Polymer Chemistry, Nankai University, Tianjin 300071, China
[b] Beijing Institute of Pharmacology and Toxicology, 27 Taiping Road, Beijing 100850, China

ABSTRACT

Folate-conjugated micelles were fabricated from amphiphilic diblock copolymers with poly(ethylene glycol) as the hydrophilic block and a random copolymer of *n*-butyl methacrylate and methacrylic acid as the hydrophobic block. Doxorubicin (DOX), a model drug that contains an amine group and hydrophobic moiety, was loaded with a high loading capacity into micelles by a combination of ionic bonding and hydrophobic effect. The combined interactions imparted a pH-sensitive delivery property to the system. The release rate of loaded DOX was slow at pH 7.4 (i.e., mimicking the plasma environment) but increased significantly at acidic pH (i.e., mimicking endosome/lysosome conditions). Acid-triggered drug release resulted from the carboxylate protonation of poly(methacrylic acid), which dissociated the ionic bonding between the micelles and DOX. Cellular uptake by folate receptor-overexpressing HeLa cells of the DOX-loaded folate-conjugated micelles was higher than that of micelles without folate conjugation. Thus, the DOX-loaded folate-conjugated micelles displayed higher cytotoxicity to HeLa cells.

© 2013 Elsevier Ltd. All rights reserved.

1. Introduction

Many therapeutic agents, while pharmacologically effective, also exhibit side-effects because of their toxicities. Meanwhile, many barriers exist for the delivery of therapeutic agents to target sites, such as renal clearance of small molecular therapeutic agents and pumping of drugs out of cells by overexpressed tumor cell membrane-associated multidrug resistance proteins [1,2]. To overcome these limitations, nanometer-sized drug carriers, such as polymer-drug conjugates, dendrimers, liposomes, polymeric micelles, and nanoparticles, have been exploited for targeting delivery of drugs [3,4]. These nanoparticulates can carry drugs preferentially to tumor tissues because of the enhanced permeability and retention (EPR) effect (known as passive targeting), bypass multidrug resistance in the cell membrane, and protect drugs from enzymatic degradation [5].

Recently, ligand-mediated targeting (active targeting) and stimuli-responsive delivery have been investigated extensively. Ligand-mediated targeting uses nanocarriers containing a specific surface ligand that imparts affinity for cellular receptors presented on tumor cells [6]. Ligands that have been used for active targeting to different cancers include galactose [7,8], folate [9,10], peptides

[11,12], antibodies [13,14], and aptmers [15,16]. Among these targeting ligands, folate has emerged as an optimal targeting ligand for the selective delivery of attached imaging and therapeutic agents to cancer tissues and sites of inflammation, due to its easy conjugation to nanocarriers, high affinity for the folate receptor ($K_d = 10^{-10}$ M), and limited distribution of folate receptor (FR) in normal tissues [17]. The chemical properties of materials sensitive to changes in biological and environmental signals, such as pH, redox potential, temperature, and specific enzymes, have been exploited in triggering drug delivery systems [18,19]. These materials should be designed to prevent premature release in the blood and normal issues. Upon reaching and accumulating in tumor tissues and/or after being taken up by cancer cells via passive or active targeting, the drugs should be rapidly released in response to the local environment.

Among the reported nanocarriers available, polymeric micelles have gained popularity in recent years due to their relative clinical success [20]. Several micellar-based drugs are currently in various stages of clinical trials for the delivery of anticancer drugs, such as doxorubicin, paclitaxel, and cisplatin [21,22]. The hydrophobic core of polymeric micelles can incorporate hydrophobic cargos by hydrophobic effect. There are several parameters that are important for using polymeric micelles as anticancer drug-delivery carriers, including a high loading capacity, extended plasma retention time, low premature release of the payload in plasma, and ability to accumulate and subsequently to release rapidly the

* Corresponding authors. Tel.: +86 22 23501705; fax: +86 22 23503510 (H. Yan), tel.: +86 10 68169362; fax: +86 10 68211656 (L. Liu).

E-mail addresses: yanhs@nankai.edu.cn (H. Yan), keliangliu@yahoo.com (K. Liu).

loaded drug in the tumor tissues or cancer cells to reach a therapeutic concentration of the drug.

Noncovalent encapsulation of drugs is a preferred method for drug delivery, due to its convenience and facile achievement compared to chemical attachment. However, the drug-loading capacities are usually low in most micellar drug delivery systems that encapsulate drugs by hydrophobic effect. In such systems, the drug-loaded core is a solid solution. The solubility of a solid solute in a hydrophobic polymeric core is usually low and depends on compatibility between the solute and core-forming block [23]. One parameter that has been used to evaluate compatibility between the polymer and solute is the Flory–Huggins interaction parameter, defined as [23]:

$$\chi_{sp} = (\delta_s - \delta_p)^2 \frac{V_s}{RT}$$

where χ_{sp} is the interaction parameter between the solute (s) and core-forming polymer block (p), δ_s is the Scatchard–Hildebrand solubility parameter of the solute, δ_p is the Scatchard–Hildebrand solubility parameter of the core-forming polymer block, and V_s is the molar volume of the solute. The lower the interaction parameter (χ_{sp}), the greater the compatibility between the solute and core-forming block. If specific (e.g., ionic) interactions are present, a very strong interaction between the solute and core-forming block may exist [23].

Doxorubicin (DOX) is an anthraquinone anticancer drug that is widely used for treatment of human malignancies. However, the therapeutic potential of DOX has been restricted by its toxicities, mainly its cardiotoxicity and myelosuppression effects, as well as multidrug resistance in cancer cells due to overexpression of P-glycoprotein [24]. To reduce the toxicity of free drug and alleviate the multidrug resistance effect, various polymeric micelles have been designed as delivery vehicles to encapsulate DOX noncovalently [8,10,13,25–42]. Most of these carriers have low DOX-loading capacities (2–10%) [8,10,13,25–31]; those with high DOX-loading capacities (>30%) usually possess either too high release rates in the plasma environment [33–41] or too low release rates in the environment of the targeted cells [41–43].

According to the Flory–Huggins interaction parameter, high loading capacities may be obtained for ionic drugs that are loaded by ionic bonding. However, drugs loaded with ionic bonding alone can be easily released by ion exchange processes in plasma, which contains 150 mM salts (mainly NaCl). For example, DOX has been loaded into nanocarriers by ionic bonding with high loading capacities; however, under such circumstances, the loaded DOX is released at a high rate in an environment mimicking plasma [36–38]. We previously showed that, compared to either ionic bonding or hydrophobic effect alone, a combination of ionic bonding and hydrophobic effect greatly enhances the binding energy of an ionic solute onto a polymeric adsorbent, due to cooperativity between the interactions [44]. In the present study, to acquire high loading capacity and endosomal/lysosomal acidic pH-triggered release, DOX, which contains an amine group, was loaded into polymeric micelles by a combination of ionic bonding and hydrophobic effect. The cores of the polymeric micelles were composed of a random copolymer of a hydrophobic monomer and a carboxylic acid group-containing monomer. The combination of ionic bonding and hydrophobic effect imparted a high affinity of DOX for the core and, thus, a high loading capacity and slow release in a neutral pH environment mimicking plasma. By choosing the carboxylic acid group-containing monomer with a proper pK_a value, the ionic interaction was dissociated in the more acidic environment of the endosomes/lysosomes, due to protonation of the carboxylate anion; thus, loaded DOX was released in a triggered fashion. In addition, the micelle surface was conjugated with folic acid as an active targeting agent. The folate-conjugated DOX-loaded micelles

showed high cellular uptake by FR-overexpressing HeLa cells and high cytotoxicity.

2. Experimental

2.1. Materials

Methoxy poly(ethylene glycol) (MPEG, 5 kDa) and poly(ethylene glycol) (PEG, 5 kDa) were purchased from Aldrich. *t*-Butyl methacrylate (*t*BMA, Acros) and *n*-butyl methacrylate (*n*BMA, Acros) were distilled over CaH$_2$ under reduced pressure before use. 2-Bromoisobutyryl bromide and 1,1,4,7,7-pentamethyldiethylenetriamine (PMDETA) were purchased from Acros. Doxorubicin (DOX) hydrochloride was obtained from Beijing HuaFeng United Technology Co., Ltd (>98%, Beijing, China). Dimethylformamide (DMF) and dimethyl sulfoxide (DMSO) were distilled over CaH$_2$ under reduced pressure and dried over 4 Å molecular sieves. Tetrahydrofuran (THF) was purified by distillation from a purple Na/benzophenone solution. Dichloromethane (DCM) was distilled over CaH$_2$. All other chemicals were used as analytical reagents without further purification. The CellTiter 96® AQ$_{ueous}$ One Solution Cell Proliferation Assay kit [3-(4,5-Dimethylthiazol-2-yl)-5-(3- carboxymethoxyphenyl)-2-(4-sulfophenyl)-2H-tetrazolium (MTS) and phenazine methosulfate (PMS)] was purchased from Promega.

2.2. Synthesis of MPEG-b-P(nBMA-ran-MAA)

MPEG 2-bromoisobutyrate (MPEG-Br) macroinitiator was synthesized by reaction of MPEG and 2-bromoisobutyryl bromide, as reported previously [45]. Block copolymers (MPEG-*b*-P(*n*BMA-*ran*-MAA) were synthesized by initiation of a mixture of *n*BMA and *t*BMA by MPEG-Br via ATRP, followed by treating the resulting polymers with trifluoroacetic acid (TFA). Typically, CuBr (14.4 mg, 0.1 mmol) and the above-prepared MPEG-Br (0.52 g, 0.1 mmol) were added to a Schlenk flask equipped with a stir bar. After sealing with a rubber septum, the flask was evacuated and purged with nitrogen (3 cycles). Deoxygenated cyclohexanone (4 mL) was added to the flask, and the mixture was stirred until the polymer was dissolved. Deoxygenated PMDETA (17.3 mg, 0.1 mmol) was added to the flask, and the mixture was stirred until the solution changed from cloudy and colorless to clear and light green. Deoxygenated *n*BMA (2.56 g, 18 mmol) and *t*BMA (1.42 g, 10 mmol) were added to the flask, and the mixture was stirred for 10 min. The flask was immersed in a water bath preheated to 60 °C. Polymerization was carried out for 10 h with stirring. The resulting mixture was diluted with dichloromethane (10 mL) and filtered through a column packed with neutral alumina to remove the catalyst. The filtrate was concentrated by rotary evaporation under reduced pressure. The polymer was precipitated into methanol/H$_2$O (1/4, v/v) and dried to get the precursor polymer MPEG-*b*-P(*n*BMA-*ran*-*t*BMA).

The above-prepared MPEG-*b*-P(*n*BMA-*ran*-*t*BMA) (1.0 g) was dissolved in 6 mL of dichloromethane, followed by addition of trifluoroacetic acid (2 mL). After the mixture was stirred for 4 h at room temperature, the solvent was removed by rotary evaporation under reduced pressure. The residue was dissolved in distilled water and the solution was dialyzed against distilled water in a dialysis tube with a molecular weight cut-off of 8–15 KDa until the pH of the outside liquid was neutral. The solution in the tube was lyophilized to get MPEG-*b*-P(*n*BMA-*ran*-MAA).

2.3. Synthesis of folate-conjugated block copolymer

Hetero-bifunctional PEG (α-folate-ω-2-bromoisobutyrate, FA–PEG-Br) was synthesized by reaction of PEG and 2-bromoisobutyryl

bromide in an equimolar ratio. The resulting polymer was coupled with folic acid by using N,N'-diisopropylcarbodiimide as the coupling agent, as reported previously [9]. Folate-conjugated block copolymer was synthesized by initiation of nBMA (1.54 g, 10.8 mmol) using FA–PEG-Br (0.53 g, 0.094 mmol) as initiator via ATRP through the method described above.

2.4. Preparation of DOX-loaded micelles

DOX-loaded micelles were prepared by dialysis method. Briefly, 10 mg of a block copolymer sample were dissolved in 0.5 mL of THF, and the solution was stirred for 2 h. To this solution was added dropwise a DOX solution (5 mg of DOX·HCl in 5 mL of distilled water) under stirring. The mixture was stirred overnight in a beaker opened to the atmosphere, allowing evaporation of THF. The mixture was dialyzed against deionized water for 2 h, phosphate buffer saline (PBS) (10 mM phosphate, 150 mM NaCl, pH 7.4) for 6 h, and deionized water for 6 h, with exchange of fresh media every 1 h. Finally, the micelle solution was filtered with a 0.45-μm microporous filter to eliminate the aggregated particles.

Folate-decorated micelles were prepared similarly with a mixture of MPEG-b-P(nBMA-ran-MAA)/FA–PEG-b-PnBMA (10/1, weight ratio).

2.5. Determination of drug-loading capacity and efficiency

The drug-loading capacity and encapsulation efficiency were determined spectrophotometrically. Typically, 1 mg of lyophilized DOX-loaded micelles was dissolved in 10 mL of DMSO. The DOX concentration in the solution was determined by spectrophotometry at 485 nm. The loading capacity and encapsulation efficiency were calculated with the following equations:

$$\text{Loading capacity} = \frac{\text{mass of loaded drug in micelles}}{\text{mass of polymer in micelles}} \times 100\%$$

$$\text{Encapsulation efficiency} = \frac{\text{mass of loaded drug in micelles}}{\text{mass of initially added drug}} \times 100\%$$

2.6. Size distribution and transmission electron microscopy

Size distribution of the micelles was determined by dynamic light scattering (DLS) on a BI-200SM instrument (Brookhaven, NY, USA). A solution of micelles (0.05%) was filtered with a Millipore filter (0.45 μm), and DLS was performed with a wavelength of 532 nm, temperature of 20 °C, and scattering angle of 90°. Transmission electron microscopy (TEM) was performed on a JEM-2010F transmission electron microscopy (JEOL, JAPAN). A drop of micelles was placed onto an amorphous carbon-coated 200-mesh copper grid. The sample was dried at ambient temperature before being loaded onto the microscope.

2.7. Critical micelle concentration measurements

The critical micelle concentration (CMC) of block copolymers was determined by fluorescence technique using pyrene as the fluorescence probe. Briefly, pyrene solution in acetone was added into several volumetric flasks. After evaporation of the acetone, copolymer micelle stock solution was added and diluted with PBS (pH 7.4) to obtain a final copolymer concentration of 10^{-5}–0.5 mg/mL; in all cases, the final concentration of pyrene was 6×10^{-7} M. Each mixture solution was sonicated for 6 h. The fluorescence spectra of the copolymer solutions were recorded on a fluorescence spectrometer (Hitachi 7000). Emission spectra were recorded from 350 to 400 nm with an excitation wavelength of 335 nm. The CMC was determined as the first inflection point on a plot of the intensity ratio of bands at 384 and 373 nm against the logarithm of copolymer concentration.

2.8. In vitro drug release

Drug release from the micelles was determined by dialyzing 2 mL of an aqueous solution of DOX-loaded micelles (1 mg/mL) against 50 mL of PBS (10 mM phosphate, 150 mM NaCl, pH 7.4, 5.0, or 4.0) at 37 °C, with a molecular weight cut-off of 8000–15,000 g/mol. At dialysis times of 1, 2, 3, 4, 5, 7, 9, 11, 24, and 30 h, the release medium was replaced with fresh PBS. The DOX concentration in the removed PBS was determined by UV–vis spectroscopy at 234 nm. All release studies were performed in triplicate to get a reliable average value.

2.9. Flow cytometry study

HeLa cells were cultured in RPMI 1640 medium with 5% penicillin–streptomycin and 10% fetal bovine serum (FBS) at 37 °C with 5% CO_2. After gathering cells by using a solution of 0.25% (w/v) trypsin and 0.03% (w/v) EDTA, a 200-μL sample of cells (5×10^4 cells/mL) was seeded onto a 12-well plate with 1 mL of RPMI 1640 medium. After incubation at 37 °C for 24 h, the medium was removed and the cells were washed twice with PBS (pH 7.4). Then, DOX-loaded micelles or free DOX in fresh RPMI 1640 medium were added to each well, and the plate was incubated again for 1 h. The medium was removed and the cells were washed twice with PBS (pH 7.4). A 500-μL aliquot of 0.25% (w/v) trypsin-0.03% (w/v) EDTA solution was added to each well to detach cells. The cells were dispersed in 300 μL of PBS (pH 7.4) for cytometric measurements on a FACSCalibur flow cytometer (BD Biosciences).

2.10. In vitro cytotoxicity against HeLa cells

HeLa cells were seeded onto 96-well plates at a seeding density of 1×10^4 cells/well. The medium was RPMI 1640 with 10% FBS and 5% penicillin–streptomycin. After culturing at 37 °C in a humidified atmosphere with 5% CO_2 for 1 d, the medium was replaced by fresh medium containing DOX-loaded micelles or free DOX at a series of concentrations. The plate was incubated for another 24 h, following which the cells were washed twice with PBS (pH 7.4). A solution (20 μL) containing MTS and PMS (20:1, v/v) was added to each well containing 80 μL PBS (pH 7.4). After incubation for 1 h at 37 °C in a humidified 5% CO_2 atmosphere, the absorbance at 490 nm in each well was recorded with a SpectraMax M5 microplate reader. The spectrophotometer was calibrated to zero absorbance by using culture medium without cells. The relative cell viability compared to control wells containing cell culture medium without DOX-loaded micelles. Free DOX was calculated by $[A]_{\text{test}}/[A]_{\text{control}}$, where $[A]_{\text{test}}$ and $[A]_{\text{control}}$ are the average absorbances of the test and control samples, respectively.

2.11. Confocal laser-scanning microscopy

HeLa cells were seeded onto 22-mm coverslips in a 6-well plate with RPMI 1640 medium and incubated for 24 h. Medium was removed, and cells were washed twice with PBS (pH 7.4). Then, DOX-loaded micelles or free DOX in fresh RPMI 1640 medium (2 μg DOX/mL) were added to each well, and the plate was incubated for 1 h at 37 °C. The cells were washed twice with PBS (pH 7.4) and were visualized by confocal laser-scanning microscopy (CLSM) at excitation and emission wavelengths of 535 and 590 nm, respectively, with a Leica TCS SP5 system (Leica, Wetzler, Germany).

3. Results and discussion

3.1. Synthesis and characterization of amphiphilic block copolymers

The aim of this work was to prepare micelles in which DOX can be encapsulated by a combination of ionic bonding and hydrophobic effect, and the loaded DOX can be released in a pH-sensitive manner. Micelles were fabricated from an amphiphilic diblock copolymer of which the hydrophobic block contained carboxylic acid groups. We chose hydrophilic PEG as the hydrophilic block and poly(n-butyl methacrylate) (PnBMA) as the hydrophobic block. To introduce carboxylic acid groups into the hydrophobic block, a carboxylic acid group-containing vinyl monomer was copolymerized with nBMA by initiation with a PEG macroinitiator. The most common carboxylic acid group-containing vinyl monomers include acrylic acid and methacrylic acid. We chose the latter as the monomer, because the protonation/deprotonation of poly(methacrylic acid) (pK_a = 5.6 [46]) should be more sensitive to pH changes from blood (pH 7.4) to endosomes (pH 5–6)/lysosomes (pH 4.5–5) than that of poly(acrylic acid) (pK_a = 4.8 [46]).

Because the monomer containing free carboxylic acid group cannot be polymerized via ATRP, a precursor diblock copolymer MPEG-b-P(nBMA-ran-tBMA) was synthesized via ATRP. Fig. 1a shows the ^{1}H NMR spectrum of the copolymer with a MPEG-Br/nBMA/tBMA molar ratio of 1/180/100. The numbers of repeat units of nBMA and tBMA in the copolymer, as determined by the ^{1}H NMR spectrum, were 187 and 106, respectively. This result was based on the characteristic peaks at 3.6 ppm (−**CH₂**−**CH₂**− of MPEG), 3.9 ppm (−O−**CH₂**−

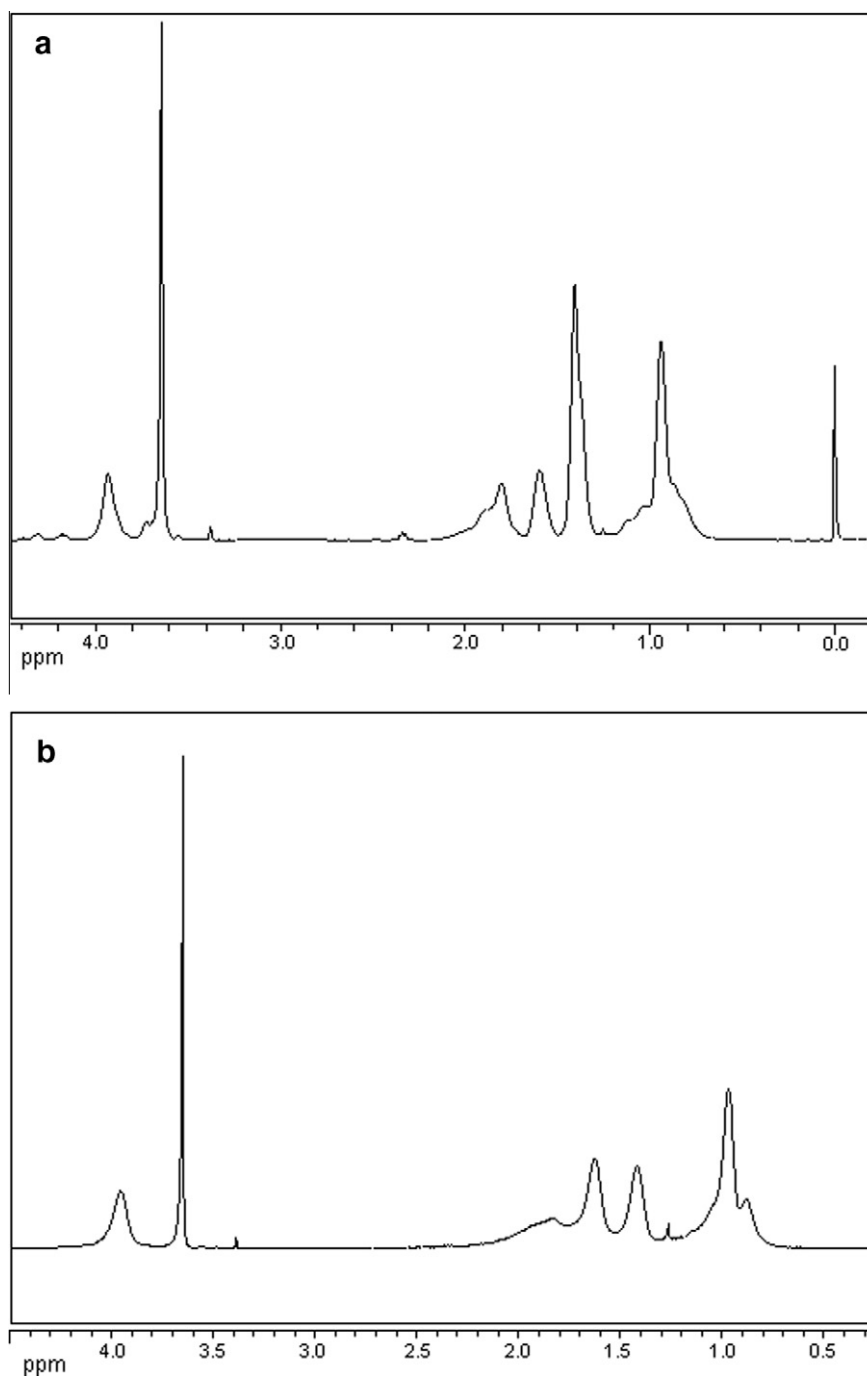**Fig. 1.** ^{1}H NMR spectra of (a) MPEG-b-P(nBMA₁₈₇-ran-tBMA₁₀₆) and (b) MPEG-b-P(nBMA₁₈₇-ran-MAA₁₀₆).

CH$_2$– of nBMA), and 1.4 ppm (–C(**CH$_3$**) of tBMA and –CH$_2$–**CH$_3$** of nBMA), using MPEG (repeat unit of 114) as the reference. This copolymer was denoted MPEG-b-P(nBMA$_{187}$-ran-tBMA$_{106}$). The molecular weight polydisperse index (M_w/M_n) of MPEG-b-P(nBMA$_{187}$-ran-tBMA$_{106}$) was determined by gel permeation chromatography to be 1.29. After removing the t-butyl groups of the tBMA units in the copolymer, the desired diblock copolymer MPEG-b-P(nBMA$_{187}$-ran-MAA$_{106}$) was obtained. The ^{1}H NMR spectrum (Fig. 1b) showed that the peak at 1.4 ppm was reduced. MPEG-b-P(nBMA$_{137}$-ran-MAA$_{168}$) and MPEG-b-P(nBMA$_{219}$-ran-MAA$_{60}$) were synthesized via a similar procedure by using the feed ratio shown in Table 1. A folate-conjugated block copolymer, FA–PEG-b-PnBMA, was also synthesized via ATRP. The synthetic processes are illustrated in Scheme 1, and the copolymer structures are shown in Table 1. In preparing the macroinitiator FA–PEG–Br from OH–PEG–OH and 2-bromoisobutyryl bromide (1:1 M ratio), three products may be generated: OH–PEG–Br, Br–PEG–Br, and unreacted OH–PEG–OH. After coupling the polymer mixture with folic acid, the polymer product should contain the desired macroinitiator FA–PEG–Br, and Br–PEG–Br and FA–PEG–FA [9]. After

initiation and propagation of nBMA by the macroinitiator, the resulting polymer mixture may contain FA–PEG-b-nBMA, nBMA-b-PEG-b-nBMA and FA–PEG–FA.

The CMCs of the amphiphilic block copolymers were determined by fluorescence technique, using pyrene as the fluorescence probe. Fig. 2 shows the plots of the fluorescence intensity ratio I_{384}/I_{373} against the logarithm of the MPEG-b-P(nBMA$_{187}$-ran-MAA$_{106}$) concentration. The first inflection point was defined as the CMC. The CMCs of micelles formed from the copolymers decreased with the decrease in the MAA repeat units in the block copolymers (Table 2). Although hydrophilic carboxylic acid groups were introduced into the block copolymers, the CMCs of these copolymers were quite low; low CMCs were especially found for MPEG-b-P(nBMA$_{187}$-ran-MAA$_{106}$) and MPEG-b-P(nBMA$_{219}$-ran-MAA$_{60}$), which contained a lower proportion of MAA units.

3.2. Preparation and characterization of DOX-loaded micelles

The DOX-loaded micelles were prepared by dialysis. An aqueous doxorubicin hydrochloride solution was added dropwise into

Table 1
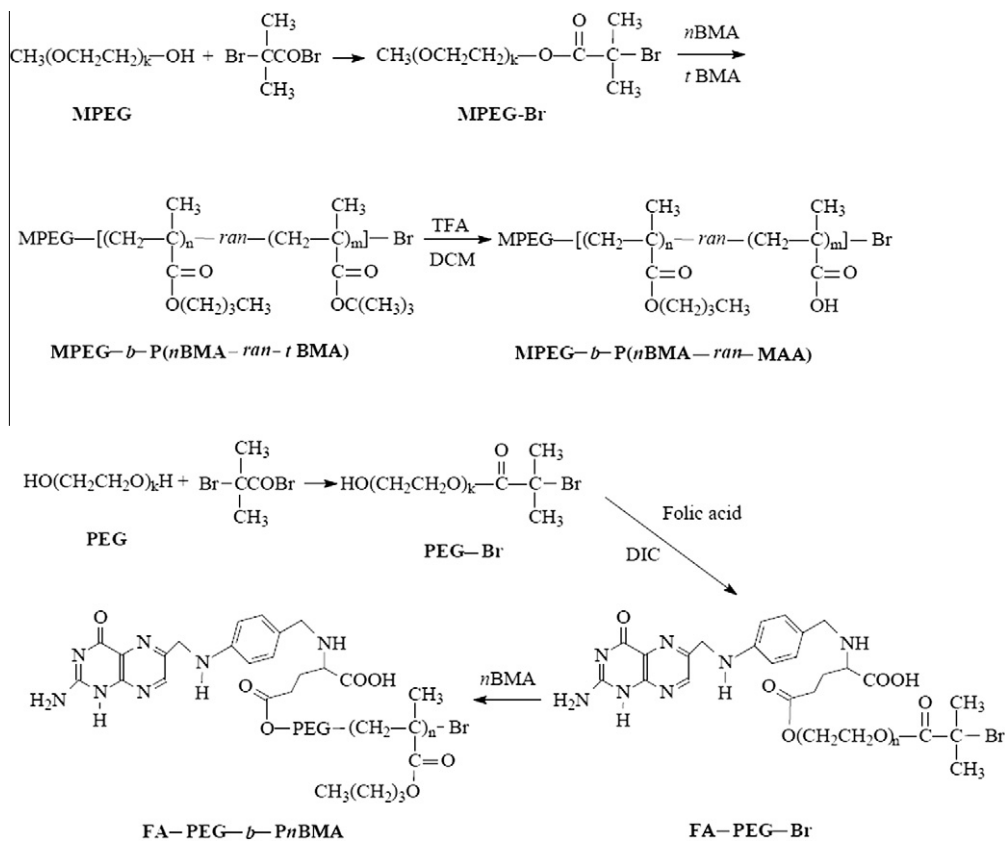Feed ratios of macroinitiator to monomers and properties of block copolymers.

Copolymer	[MI]/[M1]/M2]^a	M_n^b (kD)	M_w/M_n^c	CMC^d (μg/mL)
MPEG-b-P(nBMA$_{137}$-ran-MAA$_{168}$)	1/150/160	38.9	1.25	4.08
MPEG-b-P(nBMA$_{187}$-ran-MAA$_{106}$)	1/180/100	40.7	1.29	1.36
MPEG-b-P(nBMA$_{219}$-ran-MAA$_{60}$)	1/210/58	41.3	1.27	0.79
FA–PEG-b-PnBMA$_{119}$	1/114/0	22.4	1.30	

^{a} [MI]/[M1]/[M2], feed molar ratio of macroinitiator/monomer 1 (nBMA)/monomer 2 (tBMA).
^{b} M_n was calculated based on ^{1}H NMR of the precursor polymer MPEG-b-P(nBMA-ran-tBMA), by using PEG segment as a reference.
^{c} M_w/M_n, polydispersity index of the corresponding precursor polymer (MPEG-b-P(nBMA-ran-tBMA)) was determined by GPC.
^{d} CMC, critical micelle concentration.

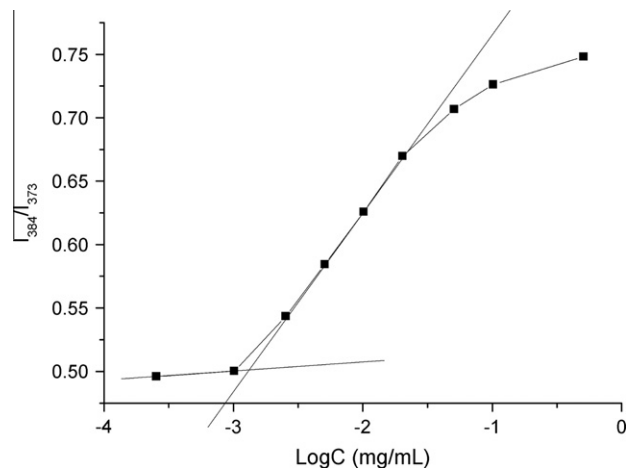**Scheme 1.** Schematic processes of block copolymer preparation.

Fig. 2. Fluorescence intensity ratio (I_{384}/I_{373}) of pyrene versus the logarithm of MPEG-b-P(nBMA$_{187}$-ran-MAA$_{106}$) micelle concentration.

Fig. 4. Size distribution of DOX-loaded MPEG-b-P(nBMA$_{187}$-ran-MAA$_{106}$) micelles in water, as determined by dynamic light scattering.

Table 2
DOX loading in micelles.

Copolymer	n_{MAA}/n_{nBMA} [a]	Loading capacity (%)	Encapsulation efficiency (%)	M_{DOX}/M_{COOH} [b]
MPEG-b-P(nBMA$_{137}$-ran-MAA$_{168}$)	1.23/1	36 ± 3	73 ± 4	0.15/1
MPEG-b-P(nBMA$_{187}$-ran-MAA$_{106}$)	0.57/1	44 ± 5	84 ± 6	0.31/1
MPEG-b-P(nBMA$_{219}$-ran-MAA$_{60}$)	0.27/1	23 ± 2	46 ± 3	0.29/1
MPEG-b-P(nBMA$_{187}$-ran-tBMA$_{106}$)		11 ± 4	22 ± 4	

[a] n_{MAA}/n_{nBMA}, ratio of the repeat units of MAA to nBMA.
[b] M_{DOX}/M_{COOH}, molar ratio of loaded DOX to carboxylic acid groups in the copolymers.

the copolymer solution in THF. After evaporation of THF, the solution was dialyzed sequentially against water, PBS (10 mM phosphate, 150 mM NaCl, pH 7.4), and water for 2, 6, and 6 h, respectively.

Fig. 3 shows the TEM image of the DOX-loaded micelles of MPEG-b-P(nBMA$_{187}$-ran-MAA$_{106}$). The micelles had a spherical morphology, with an average diameter of ~45 nm, as estimated from the TEM image. The size distribution of the micelles was
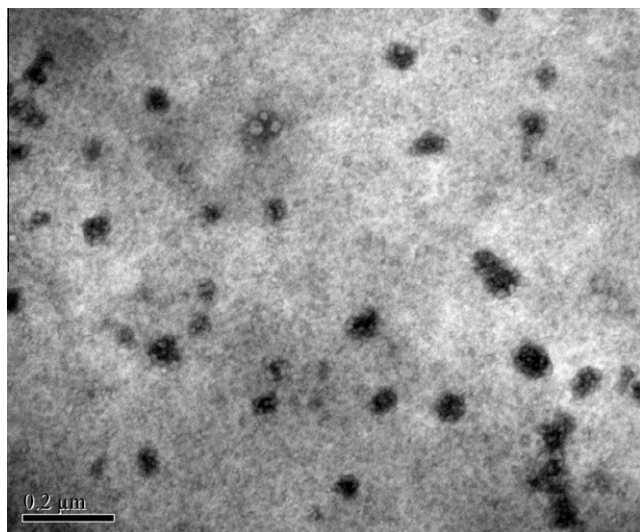

Fig. 3. TEM image of DOX-loaded MPEG-P(nBMA$_{187}$-ran-MAA$_{106}$) micelles.
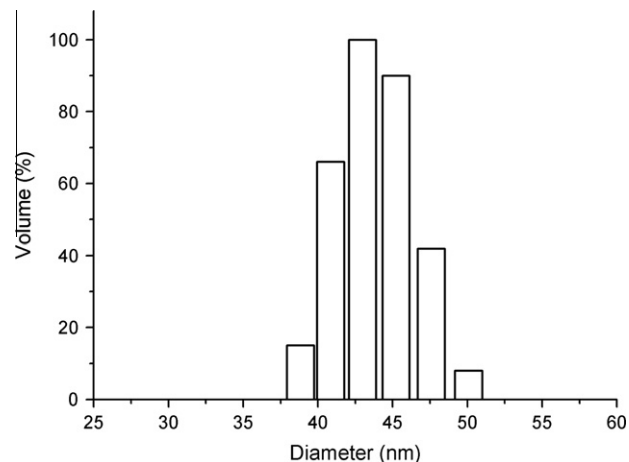
determined by DLS (Fig. 4). The average hydrodynamic diameter of the micelles was 45 nm.

Table 2 reports the DOX-loading capacities and encapsulation efficiencies. As expected, high DOX-loading capacities and encapsulation efficiencies were found for micelles formed from amphiphilic block copolymers containing carboxylic acid groups. For comparison, we determined the DOX loading capacity and encapsulation efficiency in micelles of MPEG-b-P(nBMA$_{187}$-ran-tBMA$_{106}$) that does not contain carboxylic acid groups, which is the precursor polymer of MPEG-b-P(nBMA$_{187}$-ran-MAA$_{106}$). Much lower loading capacity and encapsulation efficiency values were found in the micelles compared to those of micelles of MPEG-b-P(nBMA$_{187}$-ran-MAA$_{106}$). These results indicate that the higher loading capacity and encapsulation efficiency in micelles of block copolymers containing carboxylic acid groups can be attributed to ionic bonding between DOX and the carboxylic acid groups. At neutral pH, the carboxylic acid groups (pK_a = 5.6 [46]) of the copolymers should be deprotonated, forming anionic carboxylate, whereas the amino group of DOX (pK_a = 8.2 [47]) should be protonated, forming cationic ammonium. Thus, ionic bonds should form between the loaded DOX and anionic carboxylate.

The DOX loading in micelles of copolymers containing carboxylic acid groups was driven by ionic bonding. However, the loading capacity and encapsulation efficiency were not completely proportional to the carboxylic acid group content in the copolymers (Table 2). For example, when n_{MAA}/n_{nBMA} increased from 0.27/1 to 0.57/1, the loading capacity increased from 23% to 44%, and the encapsulation efficiency increased from 46% to 84%. However, when n_{MAA}/n_{nBMA} further increased to 1.23/1, the loading capacity and encapsulation efficiency decreased. This observation can be explained as follows: in addition to ionic bonding, loading was also driven by hydrophobic effect. Thus, a synergistic effect between the ionic bonding and hydrophobic effect should exist. It has been shown that a synergistic effect between weak interactions significantly enhances binding [44,48].

3.3. In vitro release

In vitro release of loaded DOX was studied by dialysis in PBS at different pH values at 37 °C (Fig. 5). Release from micelles of MPEG-b-P(nBMA-ran-MAA) was sensitive to the pH of the medium. The release was slow at pH 7.4: ~17% was released after 30 h from micelles containing carboxylic acid groups. Release at lower pH values (5.0 and 4.0) was much faster than that at pH 7.4. Cumulative releases from micelles of MPEG-b-P(nBMA$_{137}$-
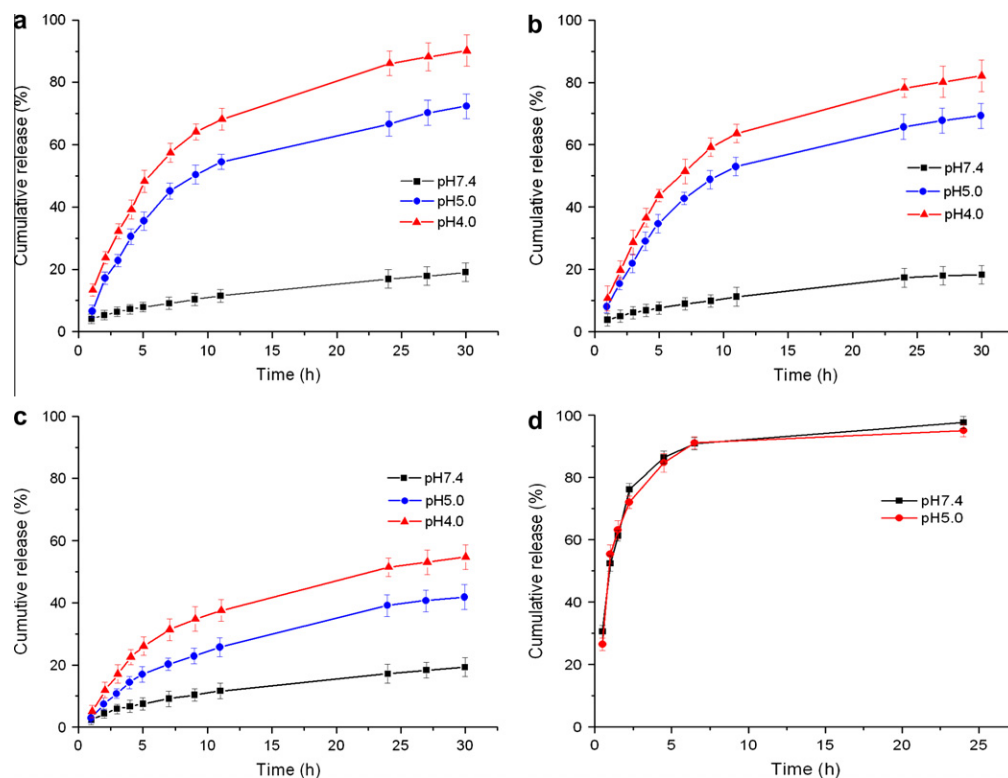
Fig. 5. DOX release in PBS (10 mM phosphate with 150 mM NaCl) at different pHs at 37 °C from the micelles of (a) MPEG-b-P(nBMA$_{137}$-ran-MAA$_{168}$), (b) MPEG-b-P(nBMA$_{187}$-ran-MAA$_{106}$), (c) MPEG-b-P(nBMA$_{219}$-ran-MAA$_{60}$), and (d) MPEG-b-P(nBMA$_{187}$-ran-tBMA$_{106}$). Results are means ± SD (n = 3).

ran-MAA$_{168}$), MPEG-b-P(nBMA$_{187}$-ran-MAA$_{106}$), and MPEG-b-P(nBMA$_{219}$-ran-MAA$_{60}$) reached 90.2%, 82.3%, and 54.6% at pH 4.0, and 72.1%, 69.2%, and 41.9% at pH 5.0, respectively, in 30 h.

The pH-sensitive release behavior can be attributed to ionic bonding between DOX and the carboxylic acid groups of the polymer. As discussed in the loading shown above, at pH 7.4, ionic bonding between the loaded DOX (pK_a = 8.2 [47]) and the carboxylic acid group (pK_a = 5.6 [46]) of the copolymers should exist; thus, the release was slow. When pH values decreased to 5.0 or 4.0, the anionic carboxylates should be protonated to form non-ionic free carboxylic acid groups. Consequently, the ionic bonding was dissociated, leading to fast release.

Hydrophobic effect between the loaded DOX and polymer should also significantly influence the release. It has been reported that 50–60% of loaded DOX was released from poly(ethylene oxide)-b-poly(methacrylic acid) nanogels after 24 h in PBS (pH 7.4) [37,38]. In these previous systems, the DOX loading should be mainly driven by ionic bonding, because the carrier did not contain hydrophobic groups. In our system, however, only ∼17% of the loaded DOX was released from the micelles after 30 h in PBS (pH 7.4) (Fig. 5a–c). This slower release behavior is consistent with the consumption that loading was driven by a combination of ionic bonding and hydrophobic effect.

No pH-sensitivity was observed for the release of loaded DOX from micelles of MPEG-b-P(nBMA$_{187}$-ran-tBMA$_{106}$) (Fig. 5d), presumably because there was no ionic bonding between the loaded DOX and the micelles. These results further demonstrate the importance of the synergistic effect between the ionic bonding and hydrophobic effect in the loading and release. An initial burst release of DOX from micelles of MPEG-b-P(nBMA$_{187}$-ran-tBMA$_{106}$) (Fig. 5d) was not expected, because the loading process included a dialysis against PBS (10 mM phosphate, 150 mM NaCl, pH 7.4), while the release at pH 7.4 was carried out in the same buffer. The burst release may be explained by the fact that the release

was performed at a higher temperature (37 °C) compared to the loading (room temperature).

3.4. Targeting of folic acid-conjugated, DOX-loaded micelles

Folic acid-conjugated and DOX-loaded micelles were prepared by self-assembly of a mixture of MPEG-b-P(nBMA$_{187}$-ran-MAA$_{106}$) and FA–PEG-b-PnBMA$_{119}$ in the presence of DOX. Tumor targeting of the folic acid-conjugated and DOX-loaded micelles (FA-micelles-DOX) was evaluated in HeLa cells, which naturally overexpress folate receptors. HeLa cells incubated with FA-micelles-DOX, DOX-loaded micelles without folate decoration (micelles-DOX), and free DOX were imaged by CLSM through the intrinsic fluorescence of DOX (Fig. 6). Cellular uptake of FA-micelles-DOX was more efficient than that of micelles-DOX, indicating that the conjugation of folate groups on the micellar surface enhanced cellular uptake. Cellular uptake of FA-micelles-DOX was even more efficient than that of free DOX, most likely due to their much more efficient cellular uptake through FR-mediated endocytosis.

Tumor targeting of the folic acid-conjugated micelles was further investigated by flow cytometry analysis. Fig. 7 shows the flow cytometry profiles of HeLa cells incubated with DOX-loaded micelles with or without folate decoration or free DOX in folate-free medium. The fluorescence intensity of cells treated with FA-micelles-DOX was much higher than those of cells treated with micelles-DOX and free DOX, consistent with the CLSM image analysis. These results further confirm the receptor-mediated uptake of folate-decorated DOX-loaded micelles.

3.5. In vitro antitumor activity

Cytotoxicity results of the DOX-loaded micelles indicated that the loaded DOX was released in HeLa cells and subsequently killed the cells (Fig. 8a). As expected, the cytotoxicity of FA-micelles-DOX
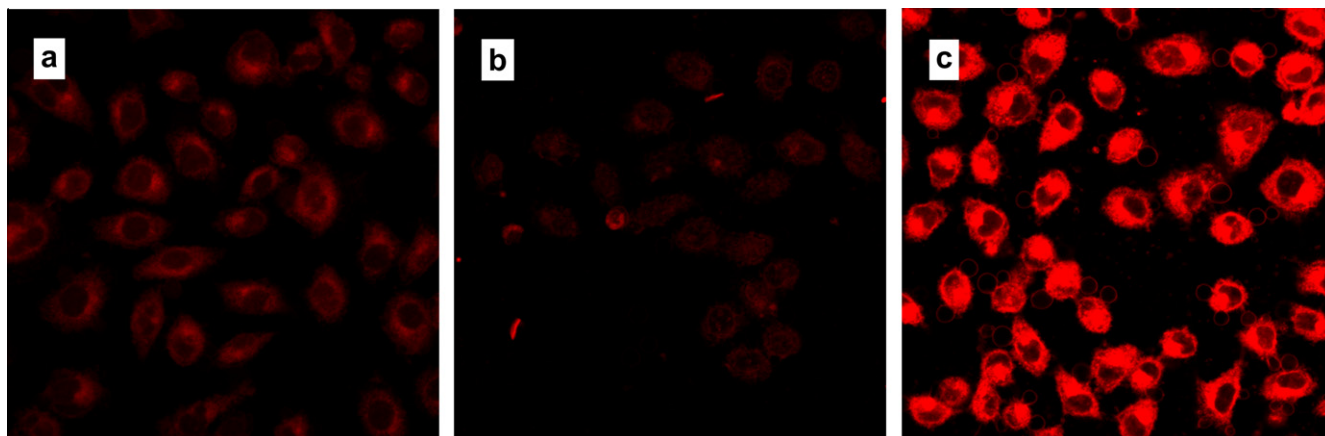
Fig. 6. Confocal laser scanning microscopy images of HeLa cells incubated with (a) free DOX, (b) micelles-DOX, and (c) FA-micelles-DOX with an equivalent DOX concentration of 10 μg/mL in each formulation in RPMI 1640 for 1 h.
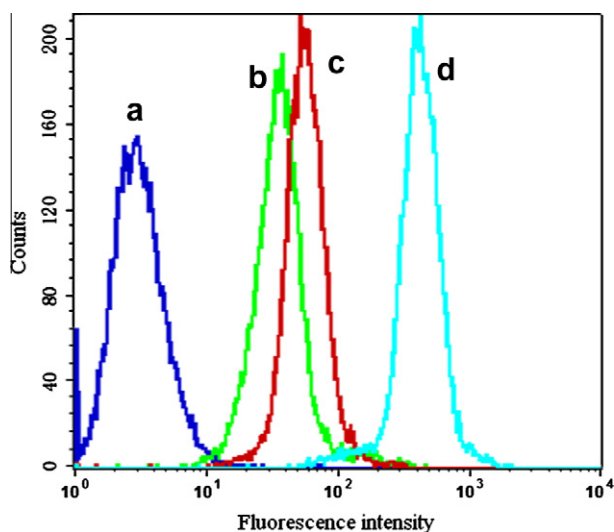

Fig. 7. Fluorescence intensities vs. cell counts when HeLa cells were exposed to (a) control, (b) micelles-DOX, (c) free DOX, and (d) FA-micelles-DOX in RPMI 1640 medium for 1 h.

Fig. 8. Viability of HeLa cells incubated with free DOX, micelles-DOX, or FA-micelles-DOX in RPMI 1640 medium. (a) Incubation time is 24 h; and (b) DOX concentration is 10 μg/ml in each formulation.

was higher than that of micelles-DOX at the same equivalent concentration of DOX, indicating that the conjugation of folate groups increased the cytotoxicity of FA-micelles-DOX. This increase appeared to be due to the specific targeting of folate-receptor on cell surfaces. Flow cytometry and CLSM analyses revealed that the cellular uptake of FA-micelles-DOX by HeLa cells was more efficient than that of free DOX, as shown above. The cytotoxicity of FA-micelles-DOX, however, was lower than that of free DOX at the same equivalent DOX concentration (Fig. 8a). This finding is most likely due to the slow DOX release rate from DOX-FA-micelles (see Fig. 5) compared to free DOX.

As mentioned above, the intracellular environment-sensitive release of DOX from the micelles was time-dependent. The time-dependent cytotoxicities of free DOX, micelles-DOX, and FA-micelles-DOX against HeLa cells were determined by incubating the cells with the drugs at 1 μg/mL DOX equivalents for various times (Fig. 8b). At incubation times of <6 h, FA-micelles-DOX displayed a similar cytotoxicity to micelles-DOX against HeLa cells, but much lower cytotoxicity than free DOX. The cytotoxicity of FA-micelles-DOX gradually became higher than that of micelles-DOX and approached that of free DOX with longer incubation times. Although the uptake of FA-micelles-DOX was even more efficient
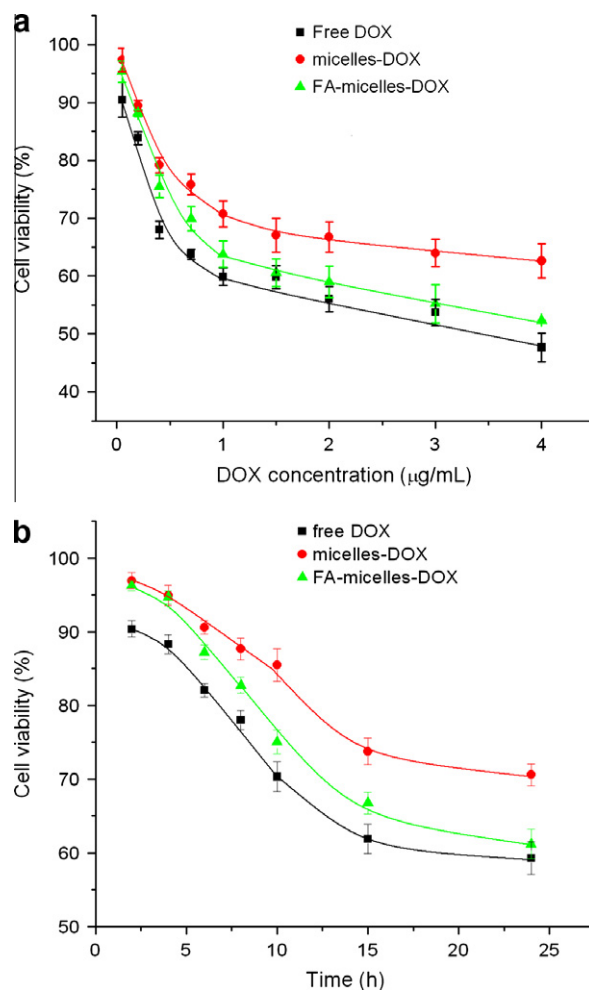
than that of free DOX, endocytosed FA-micelles-DOX only released a small quantity of the loaded DOX and exhibited a much lower cytotoxicity than free DOX at short exposure times. As the incubation time increased, more and more DOX was released. Thus, FA-micelles-DOX showed a gradually increasing cytotoxicity,

achieving a similar cytotoxicity to free DOX. These results confirm the time-dependent growth inhibitory mechanism and folate-mediated cancer cell-targeting properties of FA-micelles-DOX.

4. Conclusions

Amphiphilic diblock copolymers MPEG-*b*-P(*n*BMA-*ran*-MAA) and folate-conjugated amphiphilic diblock copolymer FA–PEG-*b*-P*n*BMA were prepared by ATRP, and DOX was loaded into micelles of MPEG-*b*-P(*n*BMA-*ran*-MAA) by dialysis. The loading capacity was high (up to 44%), because loading was driven by a combination of ionic bonding and hydrophobic effect. At neutral pH, loaded DOX was released very slowly. At more acidic pHs (i.e., mimicking endosome/lysosome conditions), the release rate significantly increased. This increase can be attributed to the protonation of polycarboxylate anions of the MAA units and, thus, dissociation of the ionic bonding between the micelles and DOX. Confocal laser scanning microscopy and flow cytometry analyses showed that the cellular uptake efficiency of the DOX-loaded folate-conjugated micelles by folate receptor-overexpressing HeLa cells was higher than those of DOX-loaded micelles without folate-conjugation and free DOX. Thus, the cytotoxicity of DOX-loaded folate-conjugated micelles was higher than that of DOX-loaded micelles without folate-conjugation and slightly lower than that of free DOX.

Acknowledgments

References

[1] J. Panyam, V. Labhasetwar, Curr. Drug Deliv. 1 (2004) 235–247.
[2] R. Perez-Tomas, Curr. Med. Chem. 13 (2006) 1859–1876.
[3] X. Wang, L. Yang, Z. Chen, D.M. Shin, CA Cancer J. Clin. 58 (2008) 97–110.
[4] M. Wang, M. Thanou, Pharm. Res. 62 (2010) 90–99.
[5] S. Modi, J.P. Jain, A.J. Domb, N. Kumar, Curr. Pharm. Des. 12 (2006) 4785–4796.
[6] M. Shi, J. Lu, M.S. Shoichet, J. Mater. Chem. 19 (2009) 5485–5498.
[7] T. Hiratsuka, M. Goto, Y. Kondo, C.S. Cho, T.R. Akaike, Macromol. Biosci. 8 (2008) 231–238.
[8] F. Suriano, R. Pratt, J.P.K. Tan, N. Wiradharma, A. Nelson, Y.Y. Yang, P. Dubois, J.L. Hedrick, Biomaterials 31 (2010) 2637–2645.
[9] M. Guo, C. Que, C. Wang, X. Liu, H. Yan, K. Liu, Biomaterials 32 (2011) 185–194.
[10] W. Zhu, Y.L. Li, L.X. Liu, W.L. Zhang, Y.M. Chen, F. Xi, J. Biomed. Mater. Res. A 96 (2011) 330–340.
[11] S. Govindarajan, J. Sivakumar, P. Garimidi, N. Rangaraj, J.M. Kumar, N.M. Rao, V. Gopal, Biomaterials 33 (2012) 2570–2582.
[12] M. Shahin, S. Ahmeda, K. Kaur, A. Lavasanifar, Biomaterials 32 (2011) 5123–5133.
[13] T. Noh, Y.H. Kook, C. Park, H. Youn, H. Kim, E.T. Oh, E.K. Choi, H.J. Park, C. Kim, J. Polym. Sci. Part A: Polym. Chem. 46 (2008) 7321–7331.
[14] S. Bhattacharyya, R.D. Singh, R. Pagano, J.D. Robertson, R. Bhattacharya, P. Mukherjee, Angew. Chem. Int. Ed. 51 (2012) 1563–1567.
[15] S. Dhar, F.X. Gu, R. Langer, O.C. Farokhzad, S.J. Lippard, Proc. Natl. Acad. Sci. USA 105 (2008) 17356–17361.
[16] A.Z. Wang, V. Bagalkot, C.C. Vasilliou, F. Gu, F. Alexis, L. Zhang, M. Shaikh, K. Yuet, M.J. Cima, R. Langer, P.W. Kantoff, N.H. Bander, S. Jon, O.C. Farokhzad, ChemMedChem 3 (2008) 1311–1315.
[17] P.S. Low, W.A. Henne, D.D. Doorneweerd, Acc. Chem. Res. 41 (2008) 120–129.
[18] F. Meng, Z. Zhong, J. Feijen, Biomacromolecules 10 (2009) 197–209.
[19] S. Ganta, H. Devalapally, A. Shahiwala, M. Amiji, J. Control. Release 126 (2008) 187–204.
[20] A.B.E. Attia, Z.Y. Ong, J.L. Hedrick, P.P. Lee, P.L.R. Ee, P.T. Hammond, Y.Y. Yang, Curr. Opin. Colloid Interface Sci. 16 (2011) 182–194.
[21] Y. Matsumura, K. Kataoka, Cancer Sci. 100 (2009) 572–579.
[22] E. Cukierman, D.R. Khan, Biochem. Pharm. 80 (2010) 762–770.
[23] C. Allen, D. Maysinger, A. Eisenberg, Colloids Surf. B: Biointerfaces 16 (1999) 3–27.
[24] D.L. Hershman, R.B. McBride, A. Eisenberger, Y.T. Wei, V.R. Grann, J.S. Jacobson, J. Clin. Oncol. 26 (2008) 3159–3165.
[25] J. Yang, E.J. Cho, S. Seo, J.W. Lee, H.G. Yoon, J.S. Suh, Y.M. Huh, S. Haam, J. Biomed. Mater. Res. A 84 (2008) 273–280.
[26] J. Park, P.M. Fong, J. Lu, K.S. Russell, C.J. Booth, W.M. Saltzman, T.M. Fahmy, Nanomedicine. NBM 5 (2009) 410–418.
[27] L.Y. Tang, Y.C. Wang, Y. Li, J.Z. Du, J. Wang, Bioconjug. Chem. 20 (2009) 1095–1099.
[28] G. Chang, C. Li, W. Lu, J. Ding, Macromol. Biosci. 10 (2010) 1248–1256.
[29] Z.Y. Qiao, R. Zhang, F.S. Du, D.H. Liang, Z.C. Li, J. Control. Release 152 (2011) 57–66.
[30] J. Liu, Y. Pang, W. Huang, X. Huang, L. Meng, X. Zhu, Y. Zhou, D. Yan, Biomacromolecules 12 (2011) 1567–1577.
[31] Z. Wu, X. Zeng, Y. Zhang, N. Feliu, P. Lundberg, B. Fadeel, M. Malkoch, A.M. Nystrom, J. Polym. Sci. Part A: Polym. Chem. 50 (2012) 217–226.
[32] K.K. Upadhyay, A.N. Bhatt, A.K. Mishra, B.S. Dwarakanath, S. Jain, C. Schatz, J.F. Le Meins, A. Farooque, G. Chandraiah, A.K. Jain, A. Misra, S. Lecommandoux, Biomaterials 31 (2010) 2882–2892.
[33] L.Y. Lin, N.S. Lee, J. Zhu, A.M. Nystrom, D.J. Pochan, R.B. Dorshow, K.L. Wooley, J. Control. Release 152 (2011) 37–48.
[34] P.L. Lu, Y.C. Chen, T.W. Ou, H.H. Chen, H.C. Tsai, C.J. Wen, C.L. Lo, S.P. Wey, K.J. Lin, T.C. Yen, G.H. Hsiue, Biomaterials 32 (2011) 2213–2221.
[35] M.S. Verma, S. Liu, Y.Y. Chen, A. Meerasa, F.X. Gu, Nano Res. 5 (2012) 49–61.
[36] Z. Liu, R. Cheung, X.Y. Wu, J.R. Ballinger, R. Bendayan, A.M. Rauth, J. Control. Release 77 (2001) 213–224.
[37] J.O. Kim, A.V. Kabanov, T.K. Bronich, J. Control. Release 138 (2009) 197–204.
[38] N.V. Nukolova, H.S. Oberoi, S.M. Cohen, A.V. Kabanov, T.K. Bronich, Biomaterials 32 (2011) 5417–5426.
[39] Y. Tian, L. Bromberg, S.N. Lin, T.A. Hatton, K.C. Tam, J. Control. Release 121 (2007) 137–145.
[40] C. Yang, J.P.K. Tan, W. Cheng, A.B.E. Attia, C.T.Y. Ting, A. Nelson, J.L. Hedrick, Y.Y. Yang, Nano Today 5 (2010) 515–523.
[41] C. Sanson, C. Schatz, J.F. Le Meins, A. Soum, J. Thevenot, E. Garanger, S. Lecommandoux, J. Control. Release 147 (2010) 428–435.
[42] W. Wang, J. Ding, C. Xiao, Z. Tang, D. Li, J. Chen, X. Zhuang, X. Chen, Biomacromolecules 12 (2011) 2466–2474.
[43] J. Yan, Z. Ye, M. Chen, Z. Liu, Y. Xiao, Y. Zhang, Y. Zhou, W. Tan, M. Lang, Biomacromolecules 12 (2011) 2562–2572.
[44] S. Cheng, H. Yan, C. Zhao, J. Chromatogr. A 1108 (2006) 43–49.
[45] S. Wan, Y. Zheng, Y. Liu, H. Yan, K. Liu, J. Mater. Chem. 15 (2005) 3424–5430.
[46] S. Fisher, R. Kunin, J. Phys. Chem. 60 (1956) 1030–1032.
[47] R.J. Sturgeon, S.G. Schulman, J. Pharm. Sci. 66 (1977) 958–961.
[48] G. Liu, H. Yu, H. Yan, Z. Shi, B. He, J. Chromatogr. A 952 (2002) 71–78.